Available online at www.sciencedirect.com
SCIENCE DIRECT®
Journal of Chromatography A, 1016 (2003) 181–193
JOURNAL OF CHROMATOGRAPHY A
www.elsevier.com/locate/chroma

Business-objective-directed, constraint-based multivariate optimization of high-performance liquid chromatography operational parameters

T.L. Chester*

Miami Valley Laboratories, The Procter & Gamble Company, P.O. Box 538707, Cincinnati, OH 45253-8707, USA

Received 11 February 2003; received in revised form 1 August 2003; accepted 4 August 2003

Abstract

The goal of a separation can be defined in terms of business needs. One goal often used is to provide the required separation in minimum time, but many other goals are also possible. These include maximizing resolution within an analysis-time limit, or minimizing the overall cost. The remaining requirements of the separation can be applied as constraints in the optimization of the goal. We will present a flexible, business-objective-based approach for optimizing the operational parameters of high performance liquid chromatography (HPLC) methods. After selecting the stationary phase and the mobile-phase components, several isocratic experiments are required to build a retention model. Multivariate optimization is performed, within the model, to find the best combination of the parameters being varied so that the result satisfies the goal to the fullest extent possible within the constraints. Interdependencies of parameters can be revealed by plotting the loci of optimal variable values or the function being optimized against a constraint. We demonstrate the concepts with a model separation originally requiring a 54 min analysis time. Multivariate optimization reduces the predicted analysis time to as short as 8 min, depending on the goals and constraints specified.

Keywords: Multivariate optimization; Optimization; Separation performance function; Cost function; Operational parameter optimization

1. Introduction

High performance liquid chromatography (HPLC) is one of the most often-used analysis techniques today. A large chemical-based business may operate hundreds of HPLC instruments. Although effort is usually spent toward optimizing HPLC methods before they are adopted for routine use, most HPLC methods are not fully optimized in the business sense we will develop in this report. Even if selectivity is optimized, we find that very large, additional savings are possible by optimizing the remaining operational parameters.

1.1. Conventional HPLC optimization

Purnell [1] showed that resolution, R_s, of a peak pair is influenced by the plate number (N), retention factors (k), and relative retention (also known as selectivity, $\alpha = k_2/k_1$ for a pair of peaks 1 and 2):

$$R_s = \frac{\sqrt{N}}{4}\frac{\alpha - 1}{\alpha}\frac{k_2}{k_2 + 1}. \quad (1)$$

* Tel.: +1-513-6272450; fax: +1-513-6271233.
E-mail address: chester.tl@pg.com (T.L. Chester).

0021-9673/$ – see front matter © 2003 Elsevier B.V. All rights reserved.
doi:10.1016/j.chroma.2003.08.005

When α and k_2 are known, Eq. (1) can be solved to determine the number of plates required, N_{req}, to achieve a given R_s:

$$N_{req} = 16R_s^2 \left(\frac{\alpha}{\alpha - 1}\right)^2 \left(\frac{k_2 + 1}{k_2}\right)^2. \quad (2)$$

The approach of sequentially adjusting k, α, and N has been taught for many years [2–4], and is often used by practitioners developing HPLC methods. However, significant performance improvement is frequently still possible after using the approach. This is so for several reasons:

1. An arbitrary goal, like resolving all peaks with a resolution of at least 2.0 and with an analysis time less than 20 min, is often stated or assumed by a worker. However, it may be ultimately possible to achieve the desired separation in much less time or with much greater resolution than stated in these goals. Alternatively, the goals, as stated, may be mutually exclusive and unachievable. It is impossible to determine, in advance, if either of these conditions will apply.
2. Experimental optimization of an HPLC separation to its ultimate performance would take dozens if not hundreds of experiments, and is such a daunting task that it is almost never done in practice. Even though many modeling tools are available to improve separations [3,5–30], many workers are content to accept marginal improvement, after only a few experiments, in order to move as rapidly as possible to actual sample analyses, especially if analysis results are needed immediately. Thus, a 25% reduction in analysis time may be considered a good return on a day of experiments to improve a method, particularly if there are thousands of samples awaiting analysis, even though the potential for much larger savings would remain unknown.
3. The approach illustrated above is an example of univariate optimization in which the three parameters (N, α, and k) contributing to resolution are assumed to be independent and are treated one at a time while holding the others constant. Univariate optimization will not work reliably, even for a simple two-parameter problem, if the parameters interact [31].
4. HPLC is even more complicated than the apparent three-parameter problem depicted in Eq. (2), and has even less chance of being effectively optimized with a univariate approach than a typical three-parameter problem because we do not have direct operational control over N, α, and k. Instead, these are influenced parametrically by the actual experimentally adjustable variables like flow rate, column length, modifier concentration, etc.

1.2. Objective functions, models, and optimization methods

Optimization generally requires selecting an objective function, then driving it to a maximum (or to a minimum in some cases) by changing one or more adjustable parameters. Siouffi and Phan-Tan-Luu [5] outlined the steps required for optimizing chromatographic methods, and summarized numerous objective functions of chromatogram quality that have been developed [3,5–15].

Optimal parameter values can be sought by numerous, single- and multi-criterion decision-making methods. These include statistical methods like Simplex [31], overlapping resolution maps [3], and various chemometric, regression, and numerical techniques [5–30].

Since experimental optimization may take dozens of trials and days or weeks of work, empirical models, derived from only a few actual chromatograms, are often used to predict the results of parameter changes [16–30]. Computer-based modeling of chromatograms has been highly developed, and several programs able to virtually simulate HPLC chromatograms and predict the effects of parameter changes are commercially available (for example [20–23]). Although many HPLC modeling programs claim to optimize chromatograms, we need to clearly distinguish *predictive capability* from *optimization*. Predictive capability can be used to virtually explore the effects of parameter changes and may be used empirically to improve chromatograms. Although accurate predictive models can replace many hours of experimental work with a few minutes of computing, optimization with this approach may be done inadvertently or deliberately in a univariate fashion, or may not include consideration of all the appropriate variables. The usual approach entails increasing the resolution or shortening the analysis time by varying either one or two parameters at a time, or may use a

factorial method or a Monte Carlo method to empirically select gradient parameters [21,22]. Lukulay and McGuffin gave a comprehensive review of HPLC optimization methods including univariate, multivariate, and parametric modulation techniques [27].

Most of these statistical and model-based methods focus on mobile-phase composition optimization (or gradient optimization) with little or no regard to efficiency parameters like flow rate and column length. In addition, many of these methods seek a compromise of conflicting goals. For example, allowing the resolution to worsen may save so much analysis time that the desirability of the resulting chromatogram, as expressed by the objective function chosen, may be preferred, even if the overlap is severe for one or more peak pairs.

1.3. Constraint-based optimization

Schoenmakers described the *minimum-criteria* optimization method in which the lowest-acceptable value of a performance parameter, such as the lowest-acceptable resolution, $R_{s,min}$, is declared [9]. The parameter space can then be searched for the parameter values meeting this constraint. A second search can be performed in the allowed parameter space to minimize retention of the last peak. Alternatively, $R_{s,min}$ can be maximized within a retention constraint. Researchers using these approaches have frequently optimized mobile-phase composition without regard to flow rate, column length, or other efficiency parameter values (for example [3,17,18]).

Cipollone et al. used the minimum-criteria approach but included several efficiency parameters in their optimization of gas chromatography parameters [19]. Their separation criterion was to resolve every peak of interest to at least some stated value. Their optimization approach then involved adjusting the chromatographic parameters to achieve this resolution constraint for the least-resolved peak pair in the chromatogram in the least amount of time possible. Thus, achieving the necessary resolution was assured, and the analysis time required to do so was minimized.

We present here a constraint-based, multivariate-optimization program for HPLC that uses business needs for directing the optimization [32]. It combines an accurate, computer-based, predictive model with a multivariate optimization specifically focusing on instrumental parameters. In operation, our goal is to identify the global optimum with respect to the parameters allowed to vary. We do not want to merely improve performance, but to quickly identify the best-possible performance that meets the business needs for the problem at hand. The selectivity parameters are picked first using any means appropriate to the problem (including any of the techniques mentioned earlier). Once the stationary phase, mobile-phase components, and other selectivity parameters have been chosen, actual data from several chromatograms must be acquired for building an empirical retention model on which the program operates to optimize the remaining variables. Extra-column effects are included in the modeling.

We distinguish separation performance functions, like resolution, from cost functions, like analysis time and volume of waste produced. In defining the required separation performance, we recognize that the resolution required may not be the same for every peak, and that performance indicators other than resolution may be preferred in some instances. Cost may be objectively expressed simply as analysis time, as volume of solvent required per analysis, as actual monetary cost per analysis, or as any objective function that reflects the business costs. Constraints on pressure, flow rate, volume of waste produced, and various dimensions may also be included.

It may appear that some of these requirements are potentially conflicting, but they can usually be resolved: performance requirements can be specified and then a cost-function minimized, or a cost-function limit can be stated and a performance function maximized. Both approaches require defining a response function to minimize or maximize, and numerous constraint values or functions to ensure that the business needs are met. Either approach gives us the unique ability to flexibly define the business needs and limits, and then seek the corresponding global optimum with respect to the adjustable parameters included in the model. If both a separation performance function and a cost function are constrained, then some problems will not have a solution.

2. Experimental

All work was performed on two similar systems, both Alliance Model 2690 HPLC systems (Waters,

Milford, MA). Either a Waters Symmetry C-18 column, 4.6 mm × 15 cm with 5 μm packing, or a Zorbax SB-Cyano column, 4.6 mm × 15 cm with 3.5 μm particles, was used. The temperature was 27 °C. The detectors in both systems were Waters 996 Photodiode Array Detectors used at 210 or 254 nm. The mobile-phase components were water (from a Milli-Q purification system, Millipore Inc., Bedford, MA, or equivalent) and HPLC-grade methanol.

Instructions for calculations were written in an Excel 2000 workbook (Microsoft Corporation, Redmond, WA) following well-established modeling methods [33]. Numerous macros were written in Microsoft Visual Basic for Applications to aid in data entry, model building, and optimization. The Excel workbook consisted of several worksheets available to users, including a main sheet depicting the current results, one containing the raw data and the retention model, and one containing the extra-column dimensions and their influences on predicted peak widths. Custom functions can be easily written and incorporated into optimizations. Optimization is done using Excel's Solver Add-In, a Generalized Reduced Gradient nonlinear optimizer. Resolution requirements for every peak, and limits on dimensions, flow rate, mobile-phase composition, pressure, in some cases maximum analysis time, and various other limits are incorporated as constraints in Solver.

Experimental data are required to build a retention model. These are collected after selecting a single column and after selecting and fixing the weak (*A*) and strong (*B*) mobile-phase components, pH, and temperature. Although we have only programmed for binary mobile phases at this point, the process does not require that *A* and *B* be pure. Either one can contain buffers, additives, or blended modifiers, if desired, as long as *A* and *B* mix without phase separation over the %*B* range of interest. The various experimental $\log k$ values for each solute are regressed against %*B*. As few as two values of %*B* may be used, but we generally use five different %*B* values and regress using a quadratic model [34]. The regression coefficients are later used to predict *k* values of each peak as a function of %*B*.

The precolumn peak transit time is calculated from the precolumn volume and the flow rate, *F*. The standard deviation of the sample (σ_{sa}, expressed in time units), by virtue of its own volume, V_{sa}, is estimated as:

$$\sigma_{sa} = \frac{V_{sa}}{\sqrt{12}F}. \quad (3)$$

Additional broadening is caused by the transport of the peak center through half its own volume out of the injector loop (only half the peak volume must be displaced to remove the peak center from the injector) plus transport through the inlet tube connecting the injector to the column. Broadening from transport through tubes is calculated using the short-tube equation of Atwood and Golay [35]:

$$\sigma_{tube} = \frac{\pi d^2 L}{4F} N^{-0.5} \left(1 + \frac{3}{N}\right)^{-0.25}, \quad (4)$$

where σ_{tube} is the standard deviation of the peak (in time units) caused by transport through a tube of diameter *d* and length *L*, and *N* the number of theoretical plates in the tube. We assume good mixing occurs in unions so that peak variances from the various parts of the HPLC instrument are additive. The temporal precolumn peak width is converted to spatial units at the column inlet by multiplying with the mobile-phase velocity on the column and dividing by $1 + k$.

Once the peaks reach the column, the basic calculation procedure follows a time-segmented approach [28–30] using 120 segments. The mobile-phase composition is calculated as a function of location on the column at each time segment. Thus, the velocity of each peak and the distance traveled are determined in each time segment, and a running record of peak position at the end of each time segment is kept. Plate height predictions are calculated using the equation of Kennedy and Knox [36], and are applied in each time segment to determine how much the peak has broadened. The peak variance in each time segment is summed with that from all preceding segments, and a running record of peak width at the end of each time segment is kept. When gradients are applied, peak widths are corrected for the effects of the gradient at every time segment using the step-gradient form of the band compression factor [37]. When the peak reaches the column outlet, the postcolumn transit time and variance are calculated and added to the values at the column outlet to predict the observed elution time and peak width. This approach is applicable to gradients of any shape. It makes no assumptions about the linearity of $\log k$ versus %*B*, nor the dependence of peak

width on the value of *k* for each peak at the column outlet. At the current state of software development, the peaks are assumed to be Gaussian shaped and symmetrical. In practice, this is not a serious oversight because the resolution requirement around a tailing peak can simply be set higher than for a normally shaped peak. (Note that the scope of this report is limited to isocratic optimization. Because both the column and mobile phase can be assumed to be uniform in space and time in isocratic HPLC, the 120-segment approach is not required. However, it does no harm other than using additional computer resources and computation time. As benefits, it provides the capability of predicting gradient chromatograms, and provides a platform for addressing gradient optimization and the use of compressible mobile phases in the future.)

Pressure is predicted empirically, beginning with the actual pressure observed within the model data and applying the proportionalities from Giddings' comprehensive flow equation [38].

The test solutes were benzyl alcohol, phenol, phenoxyethanol, potassium sorbate, benzoic acid, methylparaben, and ethylparaben, and were obtained from various commercial sources. In addition, an unknown impurity was introduced by one of the test solutes, and this impurity was included in the modeling and the optimization. Aqueous ammonium nitrate was used to mark the mobile-phase holdup time.

3. Results and discussion

3.1. Retention time and peak width accuracy

Methyl- and ethylparaben were analyzed at 40, 50, 60, 70, and 80% methanol in a water/methanol mobile phase, using the C-18 column, to build a model for testing the accuracy of predicted retention times and peak widths. This model was then assessed by comparing the predicted retention time against actual retention times for methanol concentrations of 45, 55, and 65% using the same column. The root-mean-square error in the predicted retention times was 0.007 min. When both flow rate and %*B* are changed, retention time prediction errors are less than 0.02 min over a wide range of conditions as long as the predictions are kept within the %*B* range of the original data. Predictions using %*B* values beyond the range of the original data may give reliable predictions in some cases, but the best practice to achieve high-accuracy predictions is to stay within the %*B* range of the model data.

When methanol is added to water at ambient temperature, the viscosity increases to a peak value approximately 82% higher than for pure water. Adding additional methanol then decreases the viscosity until it is 37% lower than pure water. These changes in viscosity affect the diffusion coefficients of solutes because diffusion rates are inversely proportional to solution viscosity, all else being held constant. In addition, various solutes will have different diffusion rates in the same solution due to molecular weight and molecular volume differences [39]. Therefore, values of solute diffusion coefficients vary among solutes, and these all change with HPLC conditions. Rather than keeping track of all these effects, we used a compromise value of the diffusion coefficient for all solutes and all %*B* values in the model. We typically adjust the value of this diffusion coefficient to empirically minimize the differences between the observed and predicted peak widths for the model data, and then apply this adjusted value to the subsequent prediction calculations. Using a value of 4.55×10^{-6} cm^2/s for the methyl- and ethylparaben data, the largest absolute deviation between predicted and actual peak width occurred for methylparaben with 70% methanol mobile phase: The actual 4σ-peak width, averaged from five injections, was 0.15 min, and the predicted 4σ-peak width was 0.16 min. Although the relative prediction error is 7% for this peak, the absolute error is only 0.01 min (less than 1 s). With weaker mobile phase and more strongly retained methyl- and ethylparaben peaks, the absolute errors in predicted peak widths ranged between 0.0007 and 0.006 min, or 0.1–3.5% relative to the corresponding actual peak widths for peaks as wide as 0.7 min. If a column is poorly packed and inefficient, the effective diffusion coefficient assigned in this process may be significantly different than the actual diffusion coefficient for a typical solute.

We have used this modeling approach in over 30, diverse projects so far, achieving similar results in retention time and peak width accuracy in every case. To illustrate the optimization capabilities, we will consider one data set, and show how optimal parameter values are found and how they vary depending on the approach taken and the business needs specified.

Table 1
Retention time (min)

Peak	Identity	%*B*				
		10	20	30	40	50
1	Benzyl alcohol	6.273	4.864	3.852	3.07	2.529
2	Phenol	6.785	5.354	4.221	3.294	2.647
3	Phenoxyethanol	10.352	6.861	4.852	3.541*	2.729
4	Unknown	12.668	7.737	4.919	3.541*	2.751
5	Potassium sorbate	13.698	8.737	5.822	3.952	2.887
6	Benzoic acid	16.29	10.267	6.646	4.34	3.058
7	Methylparaben	38.629	18.677	9.756	5.392	3.414
8	Ethylparaben	95.079	38.316	16.405	7.613	4.167

Retention times, as reported by the data system, observed using a Zorbax SB-Cyano column, 4.6 mm × 150 mm with 3.5 μm particles. The flow rate was 1.00 ml/min. The mobile-phase holdup time was 1.743 min. The total extra-column volume was 0.062 ml. The highest pressure observed was 19.2 MPa. The peaks marked by asterisk were not distinguishable, and the time in the table for these peaks is that reported by the data system for the apex of the merged peak.

3.2. Example model

A retention model for seven preservatives and one unknown impurity was developed using the cyano column. The retention times for the initial experiments are shown in Table 1. A retention model and a window diagram of the minimum retention factor (α_{min}) are shown in Figs. 1 and 2. For purposes of illustration, let us apply the model derived from this column to a similar column with 5 μm diameter particles but otherwise identical. The corresponding pressure for this column is 7.38 MPa (1071 psi). (When changing the column in practice, we recommend that a new retention model be developed on the specific column in use before making the final parameter adjustments.)

Among the initial experiments, the 20 %*B* trial is best, but none of the initial experiments separate all the peaks with a resolution of 2.0 or better using a 5 μm diameter particle in a 15 cm long column. Upon entering the initial retention data, the model is automatically applied to the main sheet where parameter values can be explored, and predictions and optimizations can be performed.

In most of the examples to follow, we will use 2.0 as our resolution goal around every peak. We have found that a α_{min} value of 1.08 is generally required to separate all peaks with R_s at least 2.0 if the retention factors are sufficiently high. The window diagram shows that the %*B* range available meeting this selectivity requirement is approximately 10% < %*B* < 25%. The highest α_{min} value occurs at 19 %*B*, but, with this mobile phase, the last peak to elute would have a *k* value of nearly 24. Therefore, let us arbitrarily choose 22% as our %*B* starting value because α_{min} is 1.11 (still sufficient) and because *k* for the last peak is 18.1, a

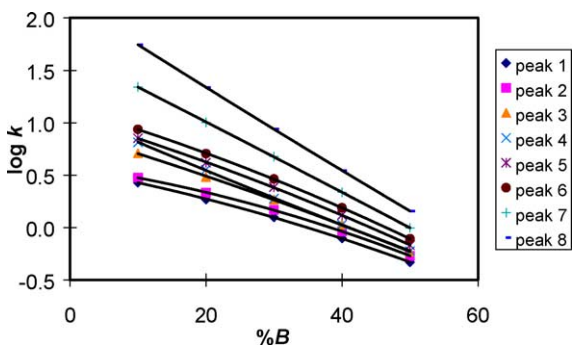

Fig. 1. The retention model for the data in Table 1.

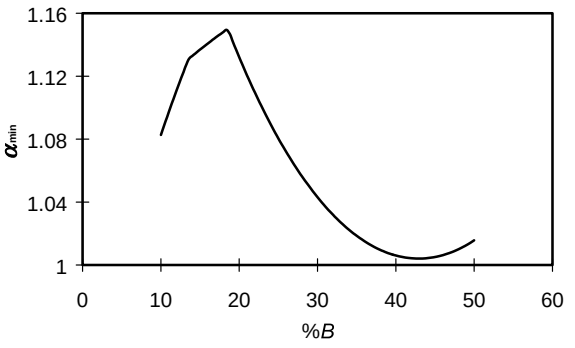

Fig. 2. The selectivity window diagram for the data in Table 1.

reduction that should save considerable time from an isocratic analysis.

3.3. Univariate optimization

From this starting point we will now illustrate the predictive capabilities of the software to explore the effects of three variables, column length (L), flow rate (F), and %B, focusing our attention on the resolution of all the peaks and the retention time of the last peak. For a fixed flow rate of 1.0 ml/min we find that a 25 cm column length separates all peaks more than adequately. The lowest R_s is 2.12 occurring between peaks 3 and 4, and the retention time for the last peak is 53.59 min. This chromatogram is shown in Fig. 3. Since we have exceeded our goal of achieving R_s values of at least 2.0, we should be able to exchange some excess resolution for a shorter analysis.

At this point, many practitioners would choose to develop a gradient method since peaks are still somewhat crowded early in the chromatogram, and are very sparse in the second half. From Fig. 3, it is easy to imagine starting a gradient at 16 min and eluting the last peak by about 23 min. With 1 min added to program the mobile phase back to the starting conditions, and 14 min (which is 4.9 column volumes at 1.00 ml/min with this column) added for re-equilibration, we would have a method capable of being cycled every 38 min. Let us reserve the possibility of using a gradient, and instead complete a univariate optimization and a multivariate optimization of this example isocratically using the software.

Using the predictive capabilities of the software to test the effects of additional parameter changes, we find that on univariately changing the column length, both 15 and 20 cm columns produce shorter analyses

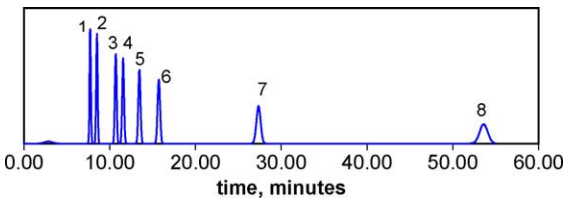

Fig. 3. This is the initial simulated chromatogram of the peaks from Table 1 following empirical adjustments to achieve or exceed the required resolution. $L = 25$ cm, $F = 1$ ml/min, %$B = 22$, and the pressure is 12.3 MPa. All resolution criteria are exceeded.

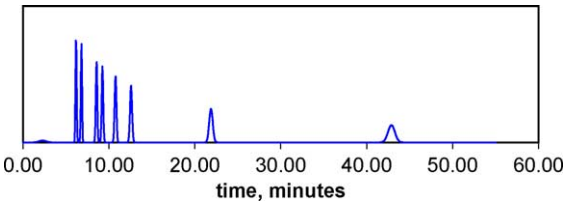

Fig. 4. The simulated chromatogram from Fig. 3 after univariate optimization. $L = 25$ cm, $F = 1.25$ ml/min, %$B = 22$, and the pressure is 15.4 MPa. All criteria are met. The elution order is the same as in Fig. 3.

but fail to meet the resolution requirement. We conclude that 25 cm is the proper length. Several trial values of flow rate then show that 1.25 ml/min shortens the retention time of the last peak to 43.87 min while meeting the resolution requirement. Increasing the %B any further, even with lowering the flow rate, does not produce a shorter analysis that still resolves all the peaks. The chromatogram at this point, Fig. 4, saves about 10 min from the chromatogram in Fig. 3. The pressure required is 15.4 MPa (2231 psi). If we were to apply a gradient at this point, in a fashion similar to that described earlier, the cycle time for injections would be about 31 min.

3.4. Multivariate minimization of analysis time

We will now illustrate using Solver to vary the same parameters, L, F, and %B, multivariately to minimize the elution time of the last peak under isocratic conditions. If we constrain the resolution around every peak to be at least 2.0, and limit the maximum flow rate to 5 ml/min and the maximum pressure to 27.6 MPa (4000 psi), then the solution requires only 26.39 min to elute the last peak while meeting all the constraints. The pressure is at the 27.6 MPa limit, $L = 24.4$ cm, $F = 2.30$ ml/min, and the mobile phase is 20.33 %B.

We have treated the column length as a continuous variable. Since a 24.4 cm column is impractical, let us test the nearest commercially available column lengths on both sides of this optimal value. Fixing the column length at a different value requires that we re-optimize the remaining parameters since their previous values correspond to the 24.4 cm column. The best solution using a 25 cm long column requires 27.22 min, 27.6 MPa, 2.24 ml/min, and 20.53 %B. The resulting chromatogram is in Fig. 5. This solution

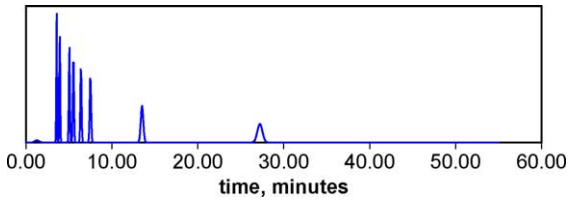

Fig. 5. The simulated chromatogram from Fig. 3 after multivariate optimization with a 27.6 MPa pressure limit. $L = 25$ cm, $F = 2.24$ ml/min, $\%B = 20.53$, and the pressure is at the limit. All criteria are met. The elution order is the same as in Fig. 3.

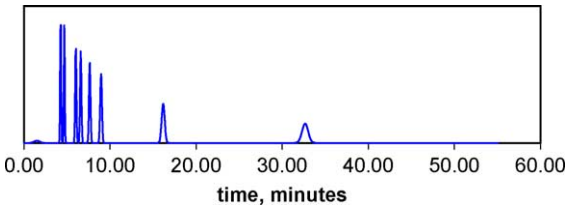

Fig. 6. The simulated chromatogram from Fig. 3 optimized for a 20 cm long column. The pressure limit was set at 15.4 MPa but the required pressure is only 14.9 MPa. $F = 1.51$ ml/min, and $\%B = 20.4$. All criteria are met. The elution order is the same as in Fig. 3.

allows an isocratic method to cycle in less time than both of the previous gradient solutions.

It appears that this solution works because the better selectivity made available by lowering %*B* from 22 reduces the plate number requirement. This allows a faster flow rate that compensates for the effect of the increase in *k* values on the analysis time. But why did the solution not use the %*B* giving the best selectivity, approximately 19%? The answer is that 19% is the best %*B* only when considered univariately, and that if we set %*B* to 19, then the higher resulting *k* values would require more time than could be made up by increasing the flow rate and shortening the column while still meeting the constraints.

The 27.6 MPa pressure in the last solution is higher than preferred by many users. Let us optimize again, this time arbitrarily choosing the pressure from our initial univariate optimization (15.4 MPa) as our upper limit. With multivariate optimization we now get a solution in which the last peak elutes in 32.26 min with $L = 20.2$ cm, $F = 1.55$ ml/min, and using 20.4 %*B*. All the resolution and pressure constraints are met. A fixed 15 cm column length requires 47.92 min at 5.7 MPa and 0.77 ml/min. With a 20 cm column the separation takes 32.65 min at 14.9 MPa and 1.51 ml/min. A 25 cm column requires 42.79 min at 15.4 MPa and 1.25 ml/min. The 20 cm long column is best for this problem, and the resulting chromatogram is shown in Fig. 6. The time required for an isocratic separation with these conditions is still comparable with the gradient solution following the earlier univariate optimization.

Except for the longest column, the pressure required in the last example was less than the pressure limit. We can gain further understanding of the complicated dependence of the optimal analysis time on the pressure limit by plotting the parameter values from a series of optimal solutions (i.e. the loci of optimal parameter values) against the pressure limit, Fig. 7. Here, we treat the column length as a continuous variable, and the figure represents the shortest possible analysis time and the corresponding values of *L*, %*B*, and *F* as a function of the pressure limit.

Fig. 7 shows that increasing the pressure limit yields a monotonic reduction in analysis time when the column length is continuously variable. This analysis-time reduction is accomplished by allowing *F* to increase as more pressure is made available. Surprisingly, *L* increases and %*B* decreases in order to go faster as the pressure limit is increased. Both of these moves (lengthening the column and weakening the mobile phase in order to go faster) are counter-intuitive, and reflect the difficulty of achieving an optimization among interdependent variables using a conventional or univariate approach.

When we restrict the column length to a few discrete values, the best column length to use is still determined by the pressure limit as shown in Fig. 8. This is a plot of best-possible analysis times against the pressure limit for 15, 20, and 25 cm columns. *F* and %*B* are not shown in the figure, but they vary in the same fashion as in Fig. 7. Below 9 MPa the 15 cm column produces the shortest analysis time, 48 min. The 15 cm column requires only 5.7 MPa to produce its best-possible result. Therefore, in this example, since the actual pressure is always lower than the pressure limit, it has no bearing on the performance of this column for this separation.

The longer columns require more pressure to achieve their optimal flow rates, and when we do not

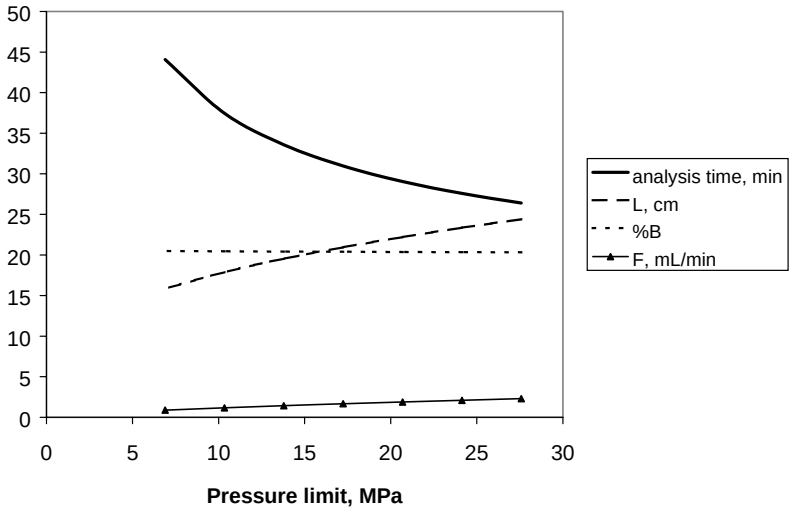

Fig. 7. Loci of the necessary analysis time and the optimal values of parameters as functions of the pressure limit. Column length is treated as a continuous variable in this plot.

provide enough pressure, both produce longer analyses than the 15 cm column. But as we increase the pressure available above 9 MPa, the 20 cm column is able to perform the analysis in less time than the 15 cm column. The 20 cm column remains pressure-limited until the pressure is allowed higher than 15 MPa. This pressure corresponds to the optimal conditions for this column, and the solution does not change further as the pressure limit is allowed to go higher.

Above 22 MPa, even faster analysis is possible using the 25 cm column. This column remains pressure-limited over the entire range of the figure.

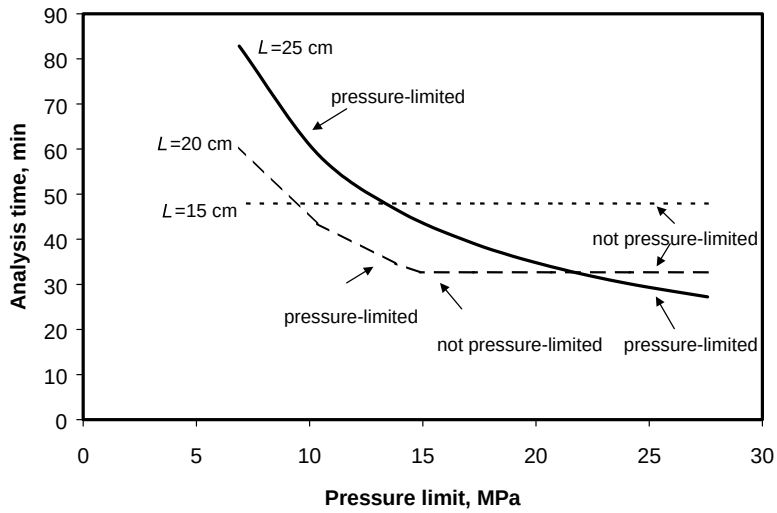

Fig. 8. Loci of the necessary analysis times for optimal conditions using 15, 20, and 25 cm long columns as a function of the pressure limit. The 15 cm column is never pressure-limited in the range of this plot. The 20 cm column is pressure-limited below 15 MPa but not above. The 25 cm column is pressure-limited everywhere. Note that the 15 cm column gives the fastest analysis when the pressure limit is below 9 MPa. Between 9 and 15 MPa the 20 cm column is fastest, and above 22 MPa the 25 cm column is fastest.

So, we see that for this problem the best column length depends on the pressure we will allow: the 15 cm column is best if the pressure must remain below 9 MPa, between 9 and 22 MPa the 20 cm column is best, and above 22 MPa the 25 cm column will produce the shortest analysis time.

Additional plots of loci of optimal parameter values against other constraints can be easily made and reveal similar interdependencies.

3.5. Maximizing resolution within given time and pressure limits

Let us suppose that our business requirement is a 30 min cycle time between successive injections. If we need 2 min beyond the last peak apex to finish the integration and to cycle the autosampler, then a reasonable business question could be, what is the best resolution possible while eluting the last peak in 28 min or less and keeping the pressure under 17.2 MPa (2500 psi)?

This requires a change in the optimization approach. Let us limit the elution time of the last peak to 28 min, and maximize the resolution around the worst peak pair. This requires us to identify the worst pair and use the resolution between these peaks as the optimization target. Any given peak pair may not always be the worst pair as conditions are explored, so let us write a custom function giving the minimum resolution among all eight peaks, and use this as the target in a maximization. (The previous R_s target values must be eliminated.)

The solution calls for $L = 19.9$ cm, $F = 1.76$ ml/min, and 20.41 %*B*. The last peak elutes in 28.0 min. The worst R_s value is 1.92 and is realized for all of the first four peaks. Using a 20 cm column gives essentially the same result.

3.6. Minimizing cost per analysis

If analysis time is not the overriding business concern, then minimizing the cost per analysis may be important. Let us assume that our costs are instrument time at US$ 50 h^{-1} and solvent at US$ 50 l^{-1}. Let us further assume we are willing to allow up to 45 min to elute the last peak. We now need a custom cost function based on time and solvent usage. With a 2 min delay between the apex of the last peak and the next injection, our cost function would be:

$$\text{cost per analysis} = (t_{R,\text{last}} + 2\,\text{min})\frac{\text{US\$ }50\,\text{h}^{-1}}{60\,\text{min/h}} + F(t_{R,\text{last}} + 2\,\text{min})\frac{\text{US\$ }50\,\text{l}^{-1}}{1000\,\text{ml/l}} \quad (5)$$

where $t_{R,\text{last}}$ is the elution time of the last peak in min, and F is in ml/min. Using this formula, the costs per analysis in Figs. 3–6 are US$ 49.11, 40.20, 27.63, and 31.50, respectively.

Recognizing that reducing the column diameter (d_c) will greatly reduce flow rate requirements, let us include the column diameter among the parameters to be varied in our cost minimization. Setting the pressure limit at 27.6 MPa we find a solution with a cost per analysis of US$ 26.69, but with a surprise: the method will run at lower cost with a larger column diameter. The best values are $L = 23.75$ cm, $d_c = 5.15$ mm, $F = 2.96$ ml/min, and 20.24 %*B*. The retention time for the last peak is 25.2 min, so our time constraint does not affect this solution. The pressure is at the 27.6 MPa limit. The increase in column diameter is driven by extra-column effects: plate numbers for the early peaks are not degraded as much by extra-column volume effects with a larger diameter column, thus allowing a faster mobile-phase velocity. This gives savings in the time-based cost that exceed the increase in solvent cost. Fixing L at 25 cm and re-optimizing the remaining parameters, the cost increases to US$ 27.38 and requires $d_c = 4.2$ mm, now smaller than the starting value. Repeating the optimization using $L = 20$ cm we find a solution costing US$ 29.09 per analysis with $d_c = 6.1$ mm. Again, this behavior reflects the interdependencies of the variables. As we saw earlier with the dependence of analysis time on the pressure limit, if we lower the pressure limit then all the parameters will have different optimal values, and the cost per analysis will increase.

3.7. Optimizing a stability-indicating method for a separation including peaks of no interest

There are often peaks in a chromatogram that are of no interest. Setting the R_s constraint on these peaks to zero can have a profound effect on the optimum conditions. This will allow these peaks to freely overlap

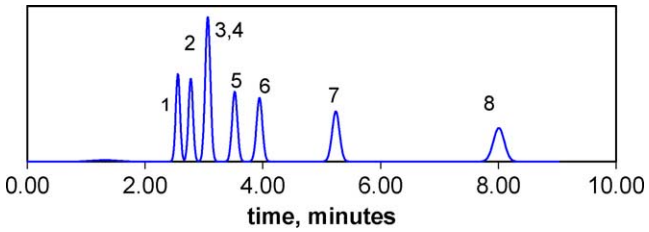

Fig. 9. The simulated chromatogram from Fig. 3 optimized for a stability-indicating assay of peak 6 with R_s constrained at 2.0 for that peak. R_s is constrained at 1.5 for peaks 2 and 5. R_s constraint values for the remaining peaks are zero. $L = 20$ cm, $F = 1.75$ ml/min, $\%B = 35.58$. All criteria are met. (Note that the time scale is different than in the earlier figures.)

with each other, but not with the peaks of interest. For example, if the R_s constraint is set to zero for peaks 3 and 4, the remaining peaks can be resolved in only 15.88 min using a 25 cm column at 1.25 ml/min with 33.9 %*B* and 15.4 MPa.

There are often more complicated situations where not all peaks of interest must be separated with the same R_s value. Let us imagine in the current example that peak 6 is our main peak of interest in a stability-indicating analysis, and that peaks 2 and 5 are degradant peaks that are not supposed to appear if the experiment is stable, and that peaks 1, 3, 4, 7, and 8 are not of interest to us as long as they do not overlap with peaks 2, 5, and 6. We can set the R_s constraint around peak 6 at 2.0 to give us a good opportunity to measure its area without interference. We may only need to recognize peaks 2 and 5 whenever they are present, so $R_s = 1.5$ is adequate for them. The R_s constraint for the remaining peaks can then be set at zero. With a pressure limit of 17.2 MPa, we get a solution taking only 8.01 min with $L = 20$ cm, $F = 1.75$ ml/min, and 35.58 %*B*, yet it fully meets the business requirements as stated. The chromatogram is shown in Fig. 9. Note that the resolution produced around peak 6 is actually 2.2, not 2.0 as constrained. This is because the resolution around peak 2 is 1.5 under these conditions, and the chromatogram cannot be eluted any faster while satisfying this constraint. A 10 min time between injections would be possible using this isocratic method.

3.8. Other possibilities

Although not illustrated above, we could include particle size among the varied parameters. If our goal is trace analysis, then we might like to achieve the best limit of detection or the best limit of quantitation possible. If we are using a mass-sensitive detector, like an evaporative light-scattering detector, then we would like to minimize the time-measured width of a target peak while achieving a stated resolution around it. This would provide separation from its neighbors while maximizing the mass flux into the mass-sensitive detector, thereby giving the best chance for detection. However, if we were using a concentration-sensitive detector we would not like to maximize the mass flux, but instead maximize the solute concentration when the peak apex is in the detector. This means minimizing the volume of the peak while achieving all the other required constraints.

We can continue writing custom functions and calculating optimal solutions with evermore-complicated constraints. For example, we could easily combine what we have seen so far to maximize resolution while specifying a maximum-allowed analysis time and a maximum-allowed analysis cost. We must be careful about setting potentially mutually exclusive constraints (such as a resolution requirement and a time limit). A solution may be possible when only one constraint of a mutually exclusive constraint pair is limiting, as we saw with the cost minimization earlier. However, if two or more mutually exclusive constraints are limiting, then Solver will not be able to find a feasible solution.

3.9. Dealing with local optima

If there is no value of %*B* that produces an α_{min} value of at least 1.08, then it is unlikely there will be a solution capable of providing $R_s > 2.0$ for all

the peaks. Alternatively, there may exist several %*B* windows capable of achieving the desired resolution. Complicated optimization problems often produce a result representing a local optimum rather than the desired global optimum. Solver is sometimes able to jump from one %*B* window into another nearby window where a better solution exists. However, Solver is not always able to jump like this, and may fail to solve the problem or may report a local optimum. If the reported solution is limited by a constraint, Solver may not be able to move around this limit even if the global optimum exists in allowed parameter space nearby.

These problems can be addressed by several means, for example, evaluating the model over a factorial grid in the space of the varied parameters to find the approximate location of the global optimum before launching Solver. We have found that this is not necessary to get useful results, and have elected not to develop the software further to do this automatically. Instead, we routinely test our solutions by starting the optimization from a variety of locations in the parameter space, making sure that we cover all the allowed parameter space in the process. If sufficient selectivity for the problem exists in multiple %*B* windows, then we will launch the optimizer from each one. If a solution is found at a constraint limit, we change one or more parameters to relieve the constraint, then start the optimization again. It immediately becomes clear if the process is getting stuck as it attempts to move along a constraint boundary.

If a constraint (like pressure) limits a solution, then the response surface may be steep with respect to one or more related parameters (like flow rate or particle size). Yet, the response surface in the neighborhood of the optimum may be quite flat with respect to one or more of the remaining parameters. The optimizer may sometimes report slightly different but essentially similar results, particularly with respect to the flat parameters, when started from different locations. In such cases, it is useful to use the predictive capabilities of the program to vary the parameters near the optimum and find out how sensitive the optimum is with respect to each variable. These efforts give much insight into the characteristics of the problem being investigated and the robustness of the result with respect to each parameter, and take only a few minutes of time at the computer.

4. Conclusion

We have demonstrated how complicated HPLC optimization is, even when only three or four parameters are varied, and how difficult it is to intuitively guess or experimentally determine optimal HPLC conditions using conventional means. However, after just a few experiments to build a model, a separation can be optimized in minutes using our approach.

Each optimization takes about 1 min to calculate on a 733 MHz computer, and each optimization reflects dozens, if not hundreds, of trial solutions. The equivalent of months of laboratory work can be done in a short computer session. The result can be an optimum based on requirements and constraints so complicated and interrelated that the optimum cannot be found experimentally in any economically reasonable fashion. As in the model we demonstrated, many problems that appear to require a gradient can be solved isocratically once all the business needs have been stated and addressed. Extension of the optimization approach shown here to gradient problems is possible.

Acknowledgements

The help and support of Jinjuin Li, S.H. Page, Rebecca Cunningham, S.O. Teremi, Kenton Juhlin, and Michael Bramley are gratefully acknowledged.

References

[1] J.H. Purnell, J. Chem. Soc. (1960) 1268.
[2] L.R. Snyder, J.J. Kirkland, Introduction to Modern Liquid Chromatography, second ed., Wiley, New York, 1979, p. 15.
[3] J.L. Glajch, J.J. Kirkland, K.M. Squire, J.M. Minor, J. Chromatogr. 199 (1980) 57.
[4] L.R. Snyder, J.J. Kirkland, J.L. Glajch, Practical HPLC Method Development, second ed., Wiley, New York, 1997, p. 1.
[5] A.M. Siouffi, R. Phan-Tan-Luu, J. Chromatogr. A 892 (2000) 75.
[6] R. Kaiser, Gas Chromatographie, Geest and Portig, Leipzig, 1960, p. 33.
[7] M.W. Watson, P.W. Carr, Anal. Chem. 51 (1979) 1835.
[8] G. D'Agostino, L. Castagnetta, F. Mitchell, M.J. O'Hare, J. Chromatogr. 338 (1985) 1.
[9] P.J. Schoenmakers, J. Chromatogr. Libr. 35 (1986) 1.
[10] O.N. Obrezkov, A.V. Pirogov, I.V. Pletnev, O.A. Shpigun, Mikrochim. Acta 1 (1991) 293.

[11] S.N. Deming, J. Chromatogr. 550 (1991) 15.
[12] M.L. Lee, S.R. Sumpter, H.D. Tolley, in: Proceedings of the 13th International Symposium on Capillary Chromatography, vol. II, Palazzo dei Congressi, Riva Del Garda, Italy, 13–16 May 1991.
[13] J. Yang, Y.-F. Chen, J. Chin. Chem. Soc. 46 (1999) 105.
[14] B. Bourguignon, D.L. Massart, Chemom. Intel. Lab. Syst. 22 (1994) 241.
[15] B. Bourguignon, D.L. Massart, J. Chromatogr. 586 (1991) 11.
[16] V. Pirogov, M.M. Platonov, I.V. Pletnev, O.N. Obrezkov, O.A. Shpigun, Anal. Chem. Acta 369 (1998) 47.
[17] P.R. Haddad, A.C.J.H. Drouen, H.A.H. Billiet, L. de Galan, J. Chromatogr. 282 (1983) 71.
[18] P.E. Kavanagh, Chromatographia 50 (1999) 65.
[19] M.G. Cipollone, T.A. Earle, J.L. Anderson, in: Proceedings of the Pittsburgh Conference on Analytical Chemistry and Applied Spectroscopy, Georgia World Congress Center, Atlanta, Georgia, 16–21 March 1997, paper 1185.
[20] A. Drouen, J.W. Dolan, L.R. Snyder, P.J. Schoenmakers, LC–GC 9 (1991) 714.
[21] S.V. Galushko, A.A. Kamenchuk, G.L. Pit, Am. Lab. 27 (1995) 33G.
[22] S.V. Galushko, A.A. Kamenchuk, LC–GC Int. 8 (1995) 581.
[23] J.W. Dolan, L.R. Snyder, N.M. Djordjevic, D.W. Hill, D.L. Saunders, L. Van Heukelem, T.J. Waeghe, J. Chromatogr. A 803 (1998) 1.
[24] Y. Hayashi, R. Matsuda, A. Nakamura, Chromatographia 30 (1990) 85.
[25] Y. Hayashi, R. Matsuda, Chromatographia 30 (1990) 171.
[26] A.-M. Dorthe, J.-L. Ramberti, A. Thienpont, Analysis 28 (2000) 587.
[27] P.H. Lukulay, V.L. McGuffin, J. Microcol. Sep. 8 (1996) 211.
[28] R.D. Smith, E.G. Chapman, B.W. Wright, Anal. Chem. 57 (1985) 2829.
[29] H. Snijders, H.G. Janssen, C. Cramers, J. Chromatogr. A 718 (1995) 339.
[30] T.L. Chester, in: Proceedings of the Third European Symposium on Analytical Supercritical Fluid Chromatography and Extraction, Uppsala, Sweden, 6–8 September 1995.
[31] F.H. Walters, L.R. Parker Jr., S.L. Morgan, S.N. Deming, Sequential Simplex Optimization, CRC Press, Boca Raton, 1991.
[32] T.L. Chester, J. Li, WO0177662A2: Methods for Modeling, Predicting, and Optimizing High Performance Liquid Chromatography Parameters, World Intellectual Property Organization, International Application Published under the Patent Cooperation Treaty, 18 October 2001.
[33] W.L. Winston, S.C. Albright, Practical Management Science: Spreadsheet Modeling and Applications, second ed., Brooks/Cole, Stamford, CT, 2003.
[34] P.J. Schoenmakers, H.A.H. Billiet, L. de Galan, J. Chromatogr. 185 (1979) 179.
[35] J.G. Atwood, M.J.E. Golay, J. Chromatogr. 218 (1981) 97.
[36] G.J. Kennedy, J.H. Knox, J. Chromatogr. Sci. 10 (1972) 549.
[37] L.R. Snyder, in: Cs. Horváth (Ed.), High-Performance Liquid Chromatography, Advances and Perspectives, vol. 1, Academic Press, New York, 1980, p. 207.
[38] J.C. Giddings, Unified Separation Science, Wiley, New York, 1991.
[39] R.C. Reid, J.M. Prausnitz, B.E. Poling, The Properties of Gases & Liquids, fourth ed., McGraw-Hill, New York, 1987.